

**INELASTIC  $J/\psi$  PHOTOPRODUCTION<sup>\*</sup>**MICHAEL KRÄMER<sup>†</sup>*Deutsches Elektronen-Synchrotron DESY, D-22603 Hamburg, FRG***Abstract**

Inelastic photoproduction of  $J/\psi$  particles at high energies is one of the processes to determine the gluon distribution in the nucleon. The QCD radiative corrections to the color-singlet model of this reaction have recently been calculated. They are large at moderate photon energies, but decrease with increasing energies. I compare the cross section and the  $J/\psi$  energy spectrum with the available fixed-target photoproduction data. Predictions for the HERA energy range are given which demonstrate the sensitivity of the result to the parametrization of the gluon distribution in the small- $x$  region.

<sup>\*</sup> Talk presented at the Workshop on "Heavy Quark Physics", Bad Honnef, FRG, Dec. 1994.

<sup>†</sup> E-mail: mkraemer@desy.de

The measurement of the gluon distribution in the nucleon is one of the important goals of lepton-nucleon scattering experiments. The classical methods exploit the evolution of the nucleon structure functions with the momentum transfer and the size of the longitudinal structure function. With rising energies, however, jet physics and the production of heavy quark states become important complementary tools. Besides open charm and bottom production, the formation of  $J/\psi$  bound states [1] in inelastic photoproduction experiments

$$\gamma + \mathcal{N} \rightarrow J/\psi + X \quad (1)$$

provides an experimentally attractive method since  $J/\psi$  particles are easy to tag in the leptonic decay modes.

Many channels contribute to the generation of  $J/\psi$  particles in photoproduction experiments [2], similar to hadroproduction experiments. However, no satisfactory quantitative picture has emerged yet and the production of a large surplus of  $\psi'$  particles in  $p\bar{p}$  collisions awaits the proper understanding. Theoretical interest so far has focussed on two mechanisms for  $J/\psi$  photo- and electroproduction, elastic/diffractive [3,4] and inelastic production through photon-gluon-fusion [1,2]. While by the first mechanism one expects to shed light on the physical nature of the pomeron, inelastic  $J/\psi$  production provides information on the distribution of gluons in the nucleon [5]. The two mechanisms can be separated by measuring the  $J/\psi$  energy spectrum, described by the scaling variable  $z = p \cdot k_\psi / p \cdot k_\gamma$  with  $p, k_\psi, \gamma$  being the momenta of the nucleon and  $J/\psi, \gamma$  particles, respectively. In the nucleon rest frame,  $z$  is the ratio of the  $J/\psi$  to the  $\gamma$  energy,  $z = E_\psi / E_\gamma$ . For elastic/diffractive events  $z$  is close to one; a clean sample of inelastic events can be obtained in the range  $z < 0.9$  [6]. The production of  $J/\psi$  particles at large transverse momenta is dominated by gluon fragmentation mechanisms [7]. Additional production mechanisms, such as  $B\bar{B}$  production and the "resolved photon" contributions at HERA can be strongly suppressed by suitable cuts [2].

Inelastic  $J/\psi$  photoproduction through photon-gluon fusion is described in the color-singlet model through the subprocess

$$\gamma + g \rightarrow J/\psi + g \quad (2)$$

shown in Fig.1. Color conservation and the Landau-Yang theorem require the emission of a gluon in the final state. The cross section is generally calculated in the static approximation in which the motion of the charm quarks in the bound state is neglected. In this approximation the production amplitude factorizes into the short distance amplitude  $\gamma + g \rightarrow c\bar{c} + g$ , with  $c\bar{c}$  in the color-singlet state and zero relative velocity of the quarks, and the  $c\bar{c}$  wave function  $\varphi(0)$  of the  $J/\psi$  bound state at the origin which is related to the leptonic width. When confronted with photoproduction data of fixed-target experiments [8,9], the theoretical predictions underestimate the measured cross section in general by more than a factor two, depending in detail on the  $J/\psi$  energy and the choice of the parameters [2]. The discrepancy with cross sections extrapolated from electroproduction data [10,11] is even larger.

The lowest-order approach to the color-singlet model demands several theoretical refinements: (i) Higher-order perturbative QCD corrections; (ii) Relativistic corrections due to the motion of the charm quarks in the  $J/\psi$  bound state; and last but not least, (iii) Higher-twist

effects which are not strongly suppressed due to the fairly low charm-quark mass. While the relativistic corrections have been demonstrated to be under control in the inelastic region [12], the problem of higher-twist contributions has not been approached so far. The calculation of the higher-order perturbative QCD corrections has been performed recently [13]. Expected *a priori* and verified subsequently, these corrections dominate the relativistic corrections in the inelastic region, being of the order of several  $\alpha_s(M_{J/\psi}^2) \sim 0.3$ . In the first step of a systematic expansion, they can therefore be determined in the static approach [14].

A detailed analysis of the  $\mathcal{O}(\alpha_s^3)$  corrections to inelastic  $J/\psi$  photoproduction is the subject of a forthcoming publication [15]; first results have been presented in Ref.[16]. In this short note the implications of the higher order QCD corrections for the partonic cross sections are discussed and the  $J/\psi$  energy spectrum is compared with the available fixed-target photoproduction data. In addition, predictions for the HERA energy range are given which demonstrate the sensitivity of the result to the parametrization of the gluon distribution in the small- $x$  region.

Generic diagrams which build up the cross section in next-to-leading order are depicted in Fig.1. Besides the usual self-energy diagrams and vertex corrections for photon and

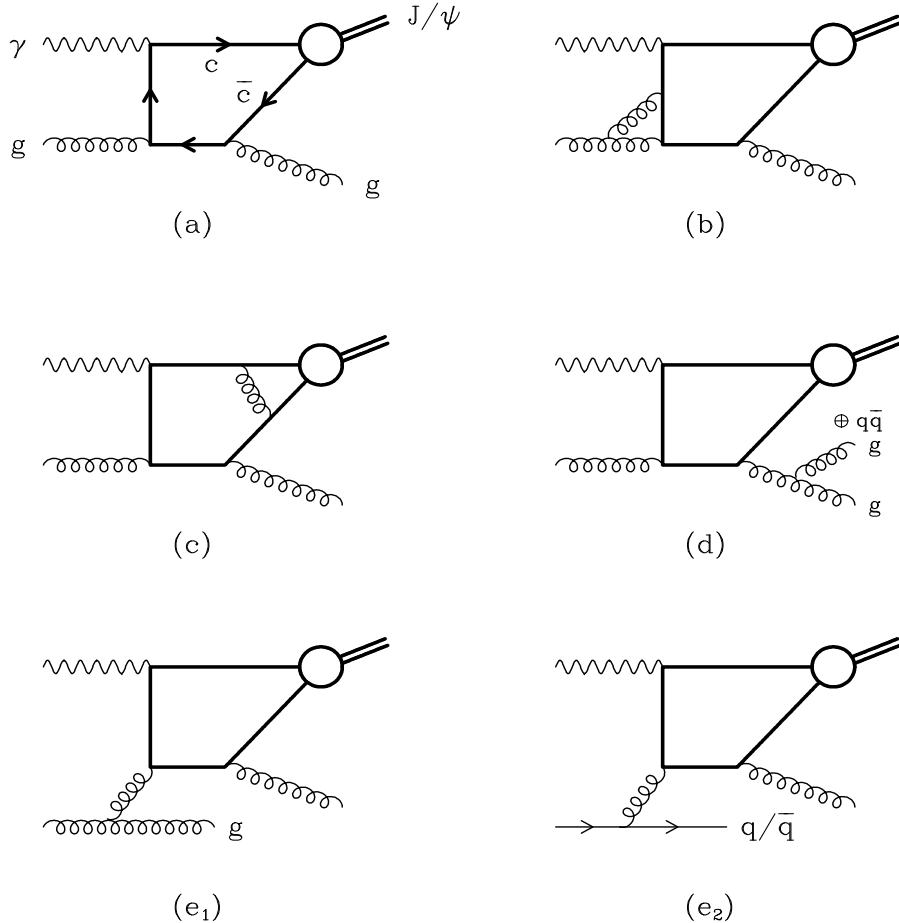


Figure 1: Generic diagrams for inelastic  $J/\psi$  photoproduction: (a) leading order contribution; (b) vertex corrections; (c) box diagrams; (d) splitting of the final state gluon into gluon or light quark-antiquark pairs; (e) diagrams renormalizing the initial-state parton densities.

gluons (b), one encounters box diagrams (c), the splitting of the final-state gluon into gluon and light quark-antiquark pairs, as well as diagrams renormalizing the initial-state parton densities (e). The evaluation of these amplitudes has been performed in the Feynman gauge and the dimensional regularization scheme has been adopted to calculate the singular parts of the amplitudes. The masses of light quarks in Fig.1(d,e<sub>1</sub>) have been neglected while the mass parameter of the charm quark has been defined on-shell. I have carried out the renormalization program in the extended  $\overline{\text{MS}}$  scheme [17] in which the massive particles are decoupled smoothly for momenta smaller than the quark mass. The exchange of Coulombic gluon quanta in the diagram (1c) leads to a Coulomb singularity  $\sim \pi^2/2\beta_R$  which can be isolated by introducing a small relative quark velocity  $\beta_R$ . Following the standard path [18], this effect has to be interpreted as the Sommerfeld rescattering correction which can effectively be mapped into the  $c\bar{c}$  wave function. As expected, the infrared singularities cancel when the emission of soft and collinear final-state gluons and light quarks, characterized by a cut-off  $\Delta$  [15,19,20], is added to the virtual corrections. The collinear initial-state singularities can be absorbed, as usual, into the renormalization of the parton densities [21] defined in the  $\overline{\text{MS}}$  factorization scheme.

The perturbative expansion of the photon-parton cross section can be expressed in terms of scaling functions,

$$\hat{\sigma}_{i\gamma}(s, m_c^2) = \frac{\alpha\alpha_s^2 e_c^2}{m_c^2} \frac{|\varphi(0)|^2}{m_c^3} \left[ c_{i\gamma}^{(0)}(\eta) + 4\pi\alpha_s \left\{ c_{i\gamma}^{(1)}(\eta) + \bar{c}_{i\gamma}^{(1)}(\eta) \ln \frac{Q^2}{m_c^2} \right\} \right] \quad (3)$$

$i = g, q, \bar{q}$  denoting the parton targets. For the sake of simplicity, I have identified the renormalization scale with the factorization scale  $\mu_R^2 = \mu_F^2 = Q^2$ . The scaling functions depend on the energy variable  $\eta = s/4m_c^2 - 1$ .  $c_{\gamma g}^{(0)}$  is the lowest-order contribution which scales  $\sim \eta^{-1} \sim 4m_c^2/s$  asymptotically.  $c_{\gamma g}^{(1)}$  can be decomposed into a "virtual + soft" (V+S) piece and a "hard" (H) gluon-radiation piece. The  $\ln^j \Delta$  singularities of the (V+S) cross section are mapped into (H), cancelling the equivalent logarithms in this contribution so that the limit  $\Delta \rightarrow 0$  can safely be carried out. The nomenclature "hard" and "virtual + soft" is therefore a matter of definition, and negative values of  $c^{(H)}$  may occur in some regions of the parameter space. Up to this order, the wave-function at the origin is related to the leptonic  $J/\psi$  width by

$$\Gamma_{ee} = \left(1 - \frac{16}{3} \frac{\alpha_s}{\pi}\right) \frac{16\pi\alpha^2 e_c^2}{M_{J/\psi}^2} |\varphi(0)|^2 \quad (4)$$

with only transverse gluon corrections taken into account explicitly [22].

The scaling functions  $c_{\gamma i}(\eta)$  are shown in Figs.2a/b for the parton cross sections integrated over  $z \leq z_1$  where I have chosen  $z_1 = 0.9$  as discussed before. [Note that the definition of  $z$  is the same at the nucleon and parton level since the momentum fraction  $\xi$  of the partons cancels in the ratio  $z = p \cdot k_\psi / p \cdot k_\gamma$ .] In the range  $0.2 \lesssim \eta \lesssim 2$  the hard gluon-radiation piece  $c_{\gamma g}^{(1,H)}$  as well as  $\bar{c}_{\gamma g}^{(1)}$  differ from the curves in Ref.[16] by a few percent since the experimental cut  $z < 0.9$  was not implemented properly in one term of [16].

The following comments can be inferred from the figures. (i) The form of the scaling functions resembles the scaling functions in open-charm photoproduction [20]. However, there is an important difference. The "virtual + soft" contribution for  $J/\psi$  production is

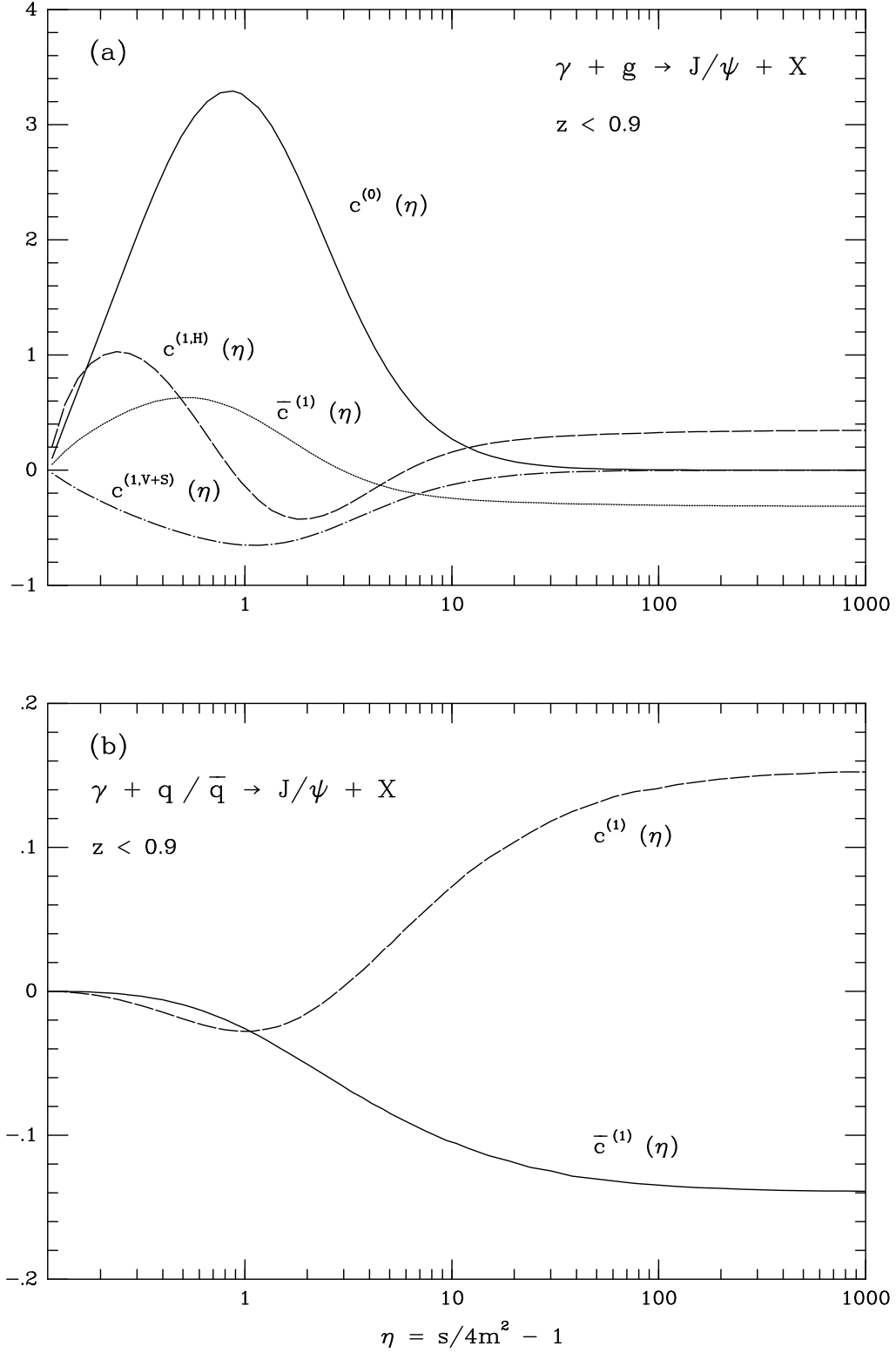


Figure 2: (a) Coefficients of the QCD corrected total inelastic  $[z < 0.9]$  cross section  $\gamma + g \rightarrow J/\psi + X$  in the physically relevant range of the scaling variable  $\eta = s_{\gamma p}/4m^2 - 1$ ; and (b) for  $\gamma + q/\bar{q} \rightarrow J/\psi + X$ .

significantly more negative than for open-charm production. The destructive interference with the lowest-order amplitude is not unplausible though, as the momentum transfer of virtual gluons has a larger chance [in a quasi-classical approach] to scatter quarks out of the small phase-space element centered at  $p_c + p_{\bar{c}} = p_{J/\psi}$  than to scatter them from outside into this small element. (ii) While  $c_{\gamma g}^{(0)}$  and  $c_{\gamma g}^{(1,V+S)}$  scale asymptotically  $\sim 1/s$ , the hard coefficients  $c_{\gamma g}^{(1,H)}$  and  $c_{\gamma q}^{(1)}$  [as well as  $\bar{c}_{\gamma g}^{(1)}$ ] approach plateaus for high energies, built-up by the flavor excitation mechanism. (iii) The cross sections on the quark targets are more than one order of magnitude smaller than those on the gluon target. (iv) A more detailed presentation of the spectra would reveal that the perturbative analysis is not under proper control in the limit  $z \rightarrow 1$ , as anticipated for this singular boundary region [15]. Outside the diffractive region, i.e. in the truly inelastic domain, the perturbation theory is well-behaved however.

The cross sections for  $J/\psi$  photoproduction on nucleons are presented in Figs.3-6. In Fig.3 the leading-order and next-to-leading order calculations are compared with the  $J/\psi$  energy spectra of the two fixed-target photoproduction experiments at photon energies near  $E_\gamma = 100$  GeV, corresponding to an invariant energy of about  $\sqrt{s_{\gamma p}} \approx 14$  GeV. The GRV

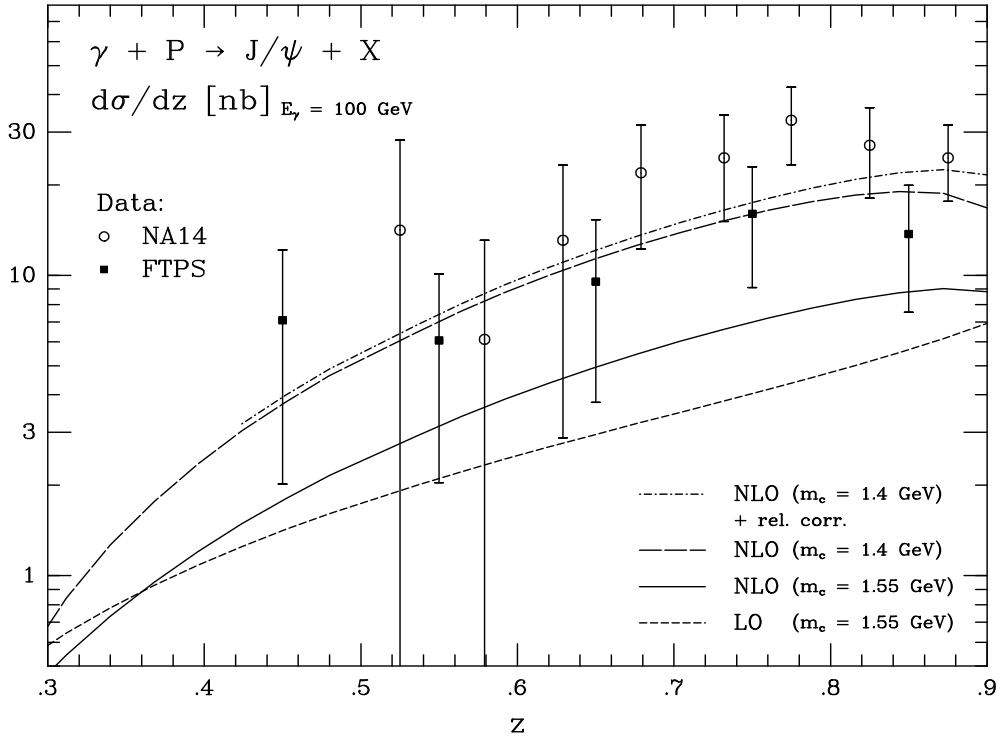


Figure 3: Energy spectrum  $d\sigma/dz$ , at the initial photon energy  $E_\gamma = 100$  GeV compared with the photoproduction data [8,9].

parametrizations of the parton densities [23] have been used. They are particularly suited to characterize the magnitude of the radiative corrections properly since they allow one to compare the results for the Born cross section folded with leading order parton densities, with the cross sections consistently evaluated for parton cross sections and parton densities in next-to-leading order. As the average momentum fraction of the partons  $\langle \xi \rangle \sim 0.1$  is moderate, the curves are not sensitive to the parametrization in the small- $x$  region. Similar to the case of open heavy flavor production [20,24], the absolute normalization of the cross section shows a strong dependence on the value of the charm quark mass. In the static

approximation the choice  $m_c = M_{J/\psi}/2$  is required for a consistent description of the heavy bound state formation. However, a smaller mass value might be appropriate for a reasonable description of the charm quark creation in the hard scattering process. In order to demonstrate this uncertainty the results are shown for two mass values,  $m_c = M_{J/\psi}/2 \approx 1.55$  GeV and  $m_c = 1.4$  GeV. The  $K$ -factor,  $K = \sigma_{\text{NLO}}/\sigma_{\text{LO}} \sim 1.5$ , consists of two parts, one due to the QCD radiative corrections of the leptonic  $J/\psi$  width [22] and a second part due to the dynamical QCD corrections [13], and does not strongly depend on  $z$ . The dependence on the renormalization/factorization scale  $Q$  is reduced considerably in next-to-leading order. While the ratio of the cross sections in leading order for  $Q = m_c : (\sqrt{2}m_c) : M_{J/\psi}$  is given by  $1.8 : 1.3 : 1$ , it is much closer to unity,  $0.7 : 1.1 : 1$ , in the next-to-leading order calculation, Fig.4. The cross section runs through a maximum [25] near  $Q \approx \sqrt{2}m_c$  with broad width,

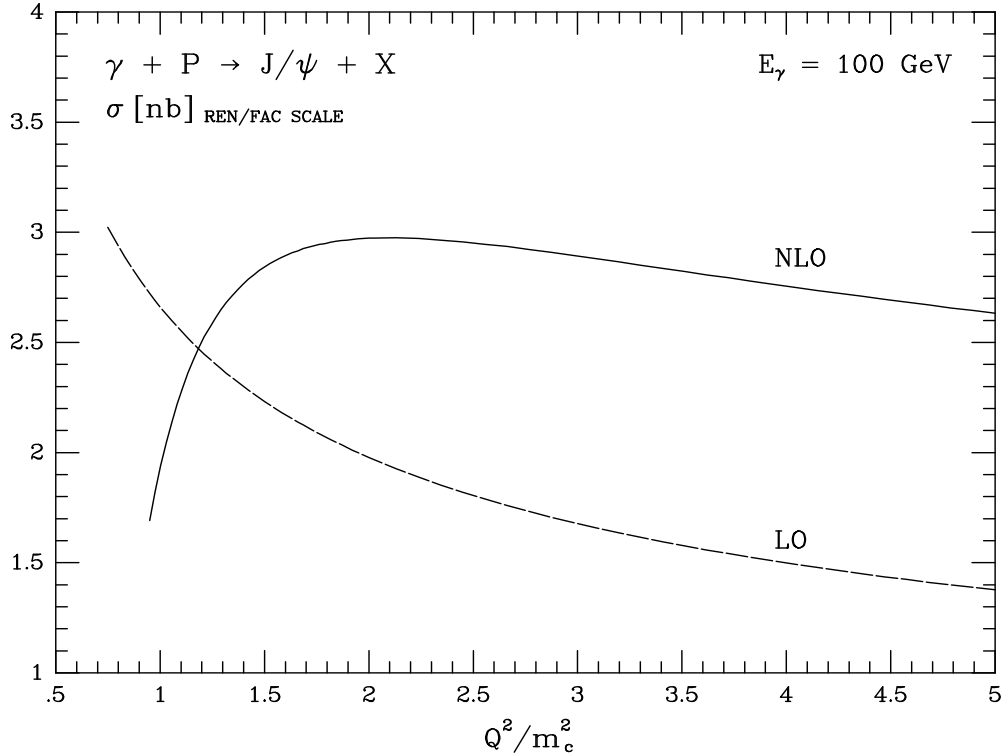


Figure 4: Dependence of the total cross section  $\gamma + P \rightarrow J/\psi + X$  on the renormalization/factorization scale  $Q$  at a photon energy of  $E_\gamma = 100$  GeV.

the origin of the stable behaviour in  $Q$ . In the BLM scheme [26]  $Q$  moves from values below  $m_c$  at low energies up to  $\sim \sqrt{2}m_c$  at the HERA energy of  $\sqrt{s_{\gamma p}} \approx 100$  GeV. In particular the value at high energies is significantly larger than the corresponding BLM value for  $J/\psi$  decays. The typical kinematical energy scale is not set any more by the small gluon energy in the  $J/\psi$  decay but rather by the typical initial-state parton energies. I have adopted the scale  $Q = \sqrt{2}m_c$  in Fig.3 and subsequently.

In a systematic expansion one may finally add the relativistic corrections as estimated in [12]. Two conclusions can be drawn from the final results presented in Fig.3. (i) The  $J/\psi$  energy dependence  $d\sigma/dz(\gamma + \mathcal{N} \rightarrow J/\psi + X)$  is adequately accounted for by the color-singlet model so that the shape of the gluon distribution in the nucleon can be extracted from  $J/\psi$  photoproduction data with confidence. (ii) The absolute normalization of the cross section is somewhat less certain; this is apparent from the comparison with the photoproduction data.

[The situation is worse for electroproduction data [10,11]]. However, allowing for higher-twist uncertainties of order  $(\Lambda/m_c)^k \lesssim 20\%$  for  $k \geq 1$ , I conclude that the normalization too appears to be under semi-quantitative control.

In Fig.5 I present the prediction of the cross section for the HERA energy range, again for two values of the charm quark mass,  $m_c = M_{J/\psi}/2$  and  $m_c = 1.4$  GeV, respectively. In

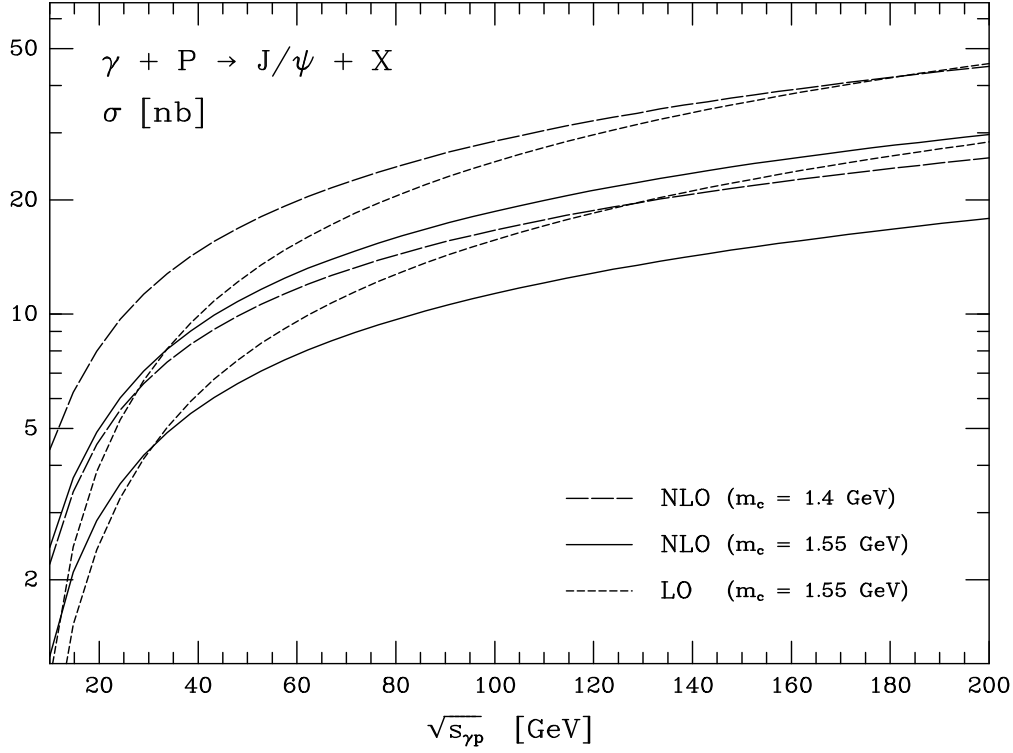


Figure 5: Total cross section for inelastic  $J/\psi$  photoproduction  $\gamma + P \rightarrow J/\psi + X$  as a function of the photon-proton center of mass energy in the HERA energy range.

this high energy range the  $K$ -factor is smaller than at low energies,  $K = \sigma_{\text{NLO}}/\sigma_{\text{LO}} \sim 0.75$ , a consequence of the negative dip in the  $c^{(1)}$  scaling function of Fig.2. Note that the LO cross section in Fig.5 has been evaluated by using leading-order expressions for the parton distributions [23]. When adopting the same set of parton distributions for both LO and NLO cross sections, the  $K$ -factor is close to one, depending in detail on the photon-proton center-of-mass energy and the choice of the parton distributions. The results in Fig.5 are shown for two values of  $\alpha_s(\sqrt{2}m_c) = 0.25$  and  $0.31$  which correspond to the  $1\sigma$  lower and upper boundary of the error band in Ref.[27], respectively. Since the cross section depends strongly on the QCD coupling, I adopt this measured value, thus allowing for a slight inconsistency to the extent that the GRV fits are based on a marginally lower value of  $\alpha_s$ . For  $m_c = M_{J/\psi}/2$  one finds, for  $z < 0.9$ , a value of about  $\sigma(\gamma + p \rightarrow J/\psi + X) \approx 18$  nb at an invariant  $\gamma p$  energy of  $\sqrt{s_{\gamma p}} \approx 100$  GeV; this value rises to about 30 nb if one chooses  $m_c = 1.4$  GeV and the larger value  $0.31$  for the QCD coupling. Inclusion of the relativistic corrections as estimated in Ref.[12] increases the cross section in the HERA energy range by approximately 10 %.

Since the momentum fraction of the partons at HERA energies is small, the cross section presented in Fig.5 is sensitive to the parametrization of the gluon distribution in the small- $x$



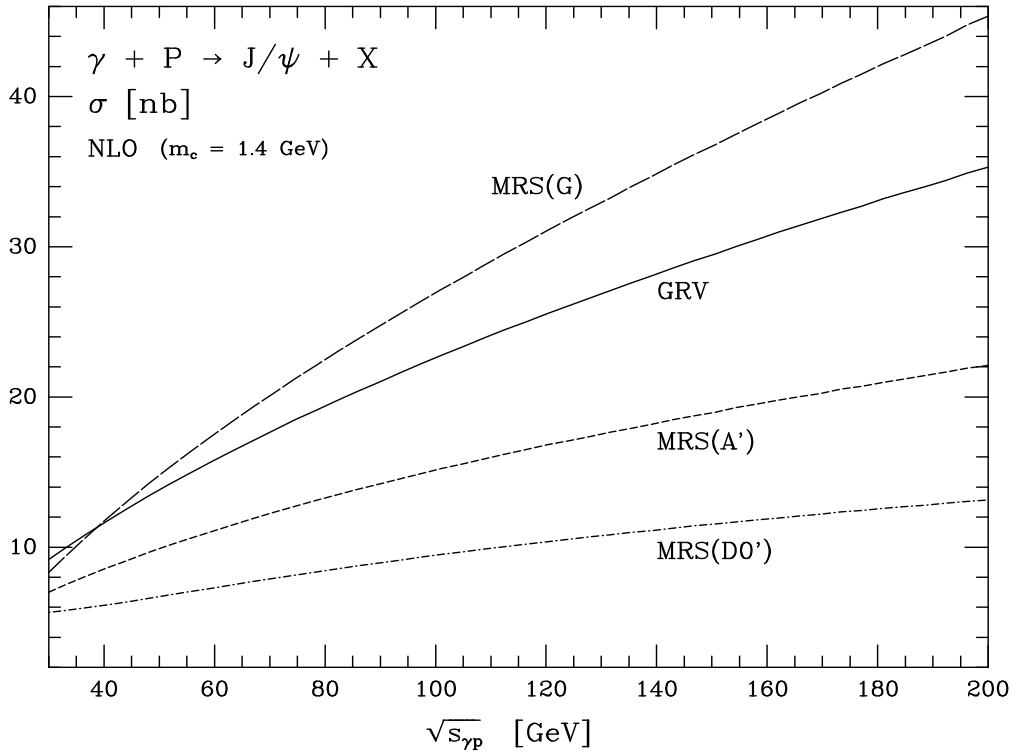


Figure 6: The total cross section as a function of the photon-proton center of mass energy for different parametrizations of the gluon distribution of the proton.

region  $\langle \xi \rangle \sim 0.003$ . This is demonstrated in Fig.6. The GRV parametrization adopted in Fig.5 leads to an almost linear rise of the cross section with the  $\gamma p$  c.m. energy. This increase is even more pronounced when using the MRS(G) set and considerably less marked for MRS(A') [28]. The MRSD0' set [29] gives rise to a much smaller cross section which does not strongly depend on the  $\gamma p$  energy in a wide range  $30 \text{ GeV} < \sqrt{s_{\gamma p}} < 200 \text{ GeV}$ . Since the absolute normalization of the cross section is rather sensitive to the value of  $\alpha_s$  and the charm quark mass, the discrimination between different parametrizations of the gluon density in the proton has to rely on the shape of the cross section [as a function of the photon-proton center of mass energy] rather than the absolute size of the prediction.

The cross sections for inelastic photoproduction of  $\psi'$  particles can be obtained from the results presented here by replacing the leptonic decay width and multiplying with a phase space correction factor,  $\sigma(\gamma P \rightarrow \psi' X) \approx \Gamma_{ee}^{\psi'}/\Gamma_{ee}^{J/\psi} (M_{J/\psi}/M_{\psi'})^3 \times \sigma(\gamma P \rightarrow J/\psi X) \approx 1/4 \times \sigma(\gamma P \rightarrow J/\psi X)$ . The production of  $\Upsilon$  bottomonium bound states is suppressed, compared with  $J/\psi$  states, by a factor of about 300 at HERA, a consequence of the smaller bottom electric charge and the phase space reduction by the large  $b$  mass.

*Conclusion:* I have shown in this next-to-leading order perturbative QCD analysis that the energy shape of the cross section for  $J/\psi$  photoproduction is adequately described by the color-singlet model. A semi-quantitative understanding has been achieved for the absolute normalization of the cross section. Higher-twist effects must be included to further improve the quality of the theoretical analysis. The predictions for the HERA energy range provide a crucial test for the underlying picture as developed so far in the perturbative QCD sector.

## Acknowledgements

It is a pleasure to thank J. Zunft for a fruitful collaboration and P.M. Zerwas for valuable discussions. I have benefitted from conversations with W.J. Stirling and A. Vogt.

## References

- [1] E.L. Berger and D. Jones, Phys. Rev. D23 (1981) 1521; R. Baier and R. Rückl, Phys. Lett. 102B (1981) 364.
- [2] H. Jung, G.A. Schuler and J. Terrón, Int. J. Mod. Phys. A7 (1992) 7955; A. Ali, Report DESY 93-105; G. Schuler, Preprint CERN-TH.7170/94.
- [3] M.G. Ryskin, Z. Phys. C57 (1993) 89; J.R. Forshaw and M.G. Ryskin, Report DESY 94-162; J.R. Cudell, Nucl. Phys. B336 (1990) 1.
- [4] T. Ahmed et al. [H1 Collaboration], Phys. Lett. 338B (1994) 507.
- [5] A.D. Martin, C.-K. Ng and W.J. Stirling, Phys. Lett. 191B (1987) 200.
- [6] R. Brugnera, private communication.
- [7] E. Braaten, M.A. Doncheski, S. Fleming and M.L. Mangano, Phys. Lett. 333B (1994) 548; M. Cacciari and M. Greco, Phys. Rev. Lett. 73 (1994) 1586; D.P. Roy and K. Sridhar, Phys. Lett. 339B (1994) 141.
- [8] R. Barate et al. [NA-14 Collaboration], Z. Phys. C33 (1987) 505.
- [9] B.H. Denby et al. [FTPS Collaboration], Phys. Rev. Lett. 52 (1984) 795.
- [10] J.J. Aubert et al. [EMC Collaboration], Nucl. Phys. B213 (1983) 1.
- [11] D. Allasia et al. [NMC Collaboration], Phys. Lett. 258B (1991) 493.
- [12] H. Jung, D. Krücker, C. Greub and D. Wyler, Z. Phys. C60 (1993) 721.
- [13] M. Krämer, PhD. Thesis, Univ. of Mainz, 1994; J. Zunft, PhD. Thesis, Univ. of Hamburg, 1994.
- [14] G.T. Bodwin, E. Braaten and G.P. Lepage, Phys. Rev. D51 (1995) 1125; T. Mannel and G. Schuler, Preprint CERN-TH.7468/94.
- [15] M. Krämer, in preparation.
- [16] M. Krämer, J. Zunft, J. Steegborn and P.M. Zerwas, Phys. Lett. 348B (1995) 657.
- [17] J. Collins, F. Wilczek and A. Zee, Phys. Rev. D18 (1978) 242; W.J. Marciano, Phys. Rev. D29 (1984) 580; P. Nason, S. Dawson and R.K. Ellis, Nucl. Phys. B303 (1988) 607.
- [18] A. Sommerfeld, Atombau und Spektrallinien, Vieweg 1939; I. Harris and L.M. Brown, Phys. Rev. 105 (1957) 1656.

- [19] W. Beenakker, H. Kuijf, W. van Neerven and J. Smith, Phys. Rev. D40 (1989) 54.
- [20] J. Smith and W.L. van Neerven, Nucl. Phys. B374 (1992) 36.
- [21] G. Altarelli, R.K. Ellis and G. Martinelli, Nucl. Phys. B157 (1979) 461.
- [22] R. Barbieri, R. Gatto and E. Remiddi, Phys. Lett. 106B (1981) 497.
- [23] M. Glück, E. Reya and A. Vogt, Preprint DO-TH 94/24, to be published in Z. Phys. C.
- [24] S. Frixione, M.L. Mangano, P. Nason and G. Ridolfi, Nucl. Phys. B431 (1994) 453; R.K. Ellis and P. Nason, Nucl. Phys. B312 (1989) 551; M. Drees, M. Krämer, J. Zunft and P.M. Zerwas, Phys. Lett. 306B (1993) 371.
- [25] P.M. Stevenson, Phys. Rev. D23 (1981) 2916.
- [26] S.J. Brodsky, G.P. Lepage and P.B. Mackenzie, Phys. Rev. D28 (1983) 228.
- [27] Particle Data Group, Phys. Rev. D50 (1994) 1173.
- [28] A.D. Martin, R.G. Roberts and W.J. Stirling, Preprint RAL-95-021.
- [29] A.D. Martin, R.G. Roberts and W.J. Stirling, Phys. Lett. 306B (1993) 145.